# Design and Analysis of 42-V Permanent-Magnet Generator for Automotive Applications

Mihai Comanescu, *Student Member, IEEE,* Ali Keyhani, *Fellow, IEEE,* and Min Dai, *Student Member, IEEE*

***Abstract*—The new 42-V automotive electric system comes up with new requirements for alternator design. A three-phase permanent-magnet (PM) synchronous generator for automotive applications is designed using analytical algorithms. The electromagnetic (EM) field for a certain design is analyzed based on a proposed equivalent magnetic circuit model. The proposed model is validated by comparing the analysis results using the model and those based on finite-element analysis under no-load and full-load conditions for saturation considerations. The analysis results demonstrate the effectiveness of the proposed machine design methodology.**

***Index Terms*—Alternators, design methodology, finite-element methods, permanent magnets (PMs), synchronous generators.**

## I. Introduction

THE ACTUAL trend in automotive design is to replace some of the mechanic and hydraulic systems with electric systems. As the cost of digital control technology keeps decreasing, the use of new electric and electronic devices is expected to provide new features and improved performance as well as increased comfort and customer satisfaction.

The actual power demand in an automobile is in the range of 1.2 to 1.5 kW. The automotive electric system in use for the last 30 years is based on the claw pole alternator also known as the Lundell machine. This is a three-phase synchronous generator equipped with a field winding and brushes. Its output voltage is applied to an ac/dc converter. The output voltage of the system is controlled by regulating the field current of the machine. Thus, no control is needed for the converter, usually a six-diode bridge rectifier. Despite the relatively low performance of the Lundell machine, this system was for many years the best compromise between efficiency and cost.

With new loads being added to the automotive power system, it is estimated that by 2005 the power demand of a typical car will be in the range of 2.5 to 3 kW. Examples of such loads are electric air conditioners, electric steering systems, electric brakes, or high-energy discharge lamps. At this level of demand, the system based on the Lundell machine and the unique 12-V dc bus voltage becomes inefficient. The losses in the alternator are significant and the increased currents require thicker wiring harnesses. The cost of the system increases while the performance drops. Considering the concern for improved fuel economy and reduced emissions, the need for an electric system with improved efficiency is apparent while the increase in cost can now be justified with energy savings. With the new level of 42 V as standard level voltage, automotive companies have started to examine the design of the electrical system and loads to ensure the transition. Various solutions for the future power system are examined in [6] and [7]. Recent advancements in permanent-magnet (PM) materials technology and the affordable price of the high-energy magnets make the PM machine an attractive solution.

Most of the PM designs in literature address motors. Pillay *et al*. [8] presents a literature survey on PM ac motors and drives showing some aspects regarding design and control. A comparative study of different designs in terms of dimensions and torque capability is presented in [1]. A general method for sizing of electric machines that highlights the need of relating the design with the type of converter used is shown in [4]. Extensive aspects of PM motor technology and design of brushless dc machines are presented in [3] and [5]. Some of these concepts are used in this paper.

This paper presents the design methodology of a three-phase PM synchronous alternator. The design algorithm as well as an equivalent magnetic circuit model of the PM machine called the "reluctance model" is presented. Input data and results are shown. The design is validated using finite-element analysis. The rated voltage and current of the machine assume the load voltage of 42 V and take into account the topology of the converter used.

## II. Problem Description

The objective of this research is the design of a three-phase PM synchronous alternator supplying 2.5 kW and 42 V to the dc loads. The speed of the alternator is in the range of 1800–18 000 r/min. The requirement is that the machine should provide rated power and voltage at idle speed (1800 r/min). The converter topology of this system consists of an uncontrolled bridge rectifier and a buck converter, as shown in Fig. 1.

This solution provides good efficiency and convenient control. At high speed, the switch of the buck converter is turned on and off such that the voltage is stepped down to the required level.

A fully controlled rectifier alone could have been used if the speed range of the application had not been that wide. As there is no control of the output voltages of the PM generator, the magnitude and frequency of the voltages increase with speed. Consequently, the firing angles of the switches must be reduced to achieve voltage regulation. Voltages and currents in the system become very pulsating at high speeds and the high rms value of the current drives the losses in the machine and converter to

Manuscript received June 12, 2000; revised January 10, 2002. This work was supported by Delphi Automotive Systems and Magsoft Corporation.

The authors are with the Department of Electrical Engineering, The Ohio State University, Columbus, OH 43210 USA (e-mail: comanesm@ee.eng.ohio-state.edu; keyhani@ee.eng.ohio-state.edu; daim@ee.eng.ohio-state.edu).

Digital Object Identifier 10.1109/TEC.2002.808380

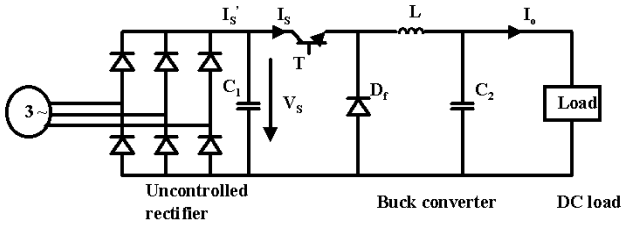


Fig. 1. Uncontrolled six-diode bridge rectifier and buck converter.

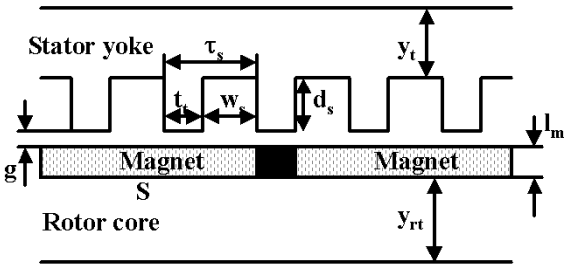


Fig. 2. Machine structure.

an unacceptable level. In an uncontrolled rectifier, each diode is conducting for 120 electrical degrees and the problem of the pulsating currents is reduced. Moreover, the LC structure of the buck converter represents a filter by itself; consequently, the voltage and current waveforms are improved.

The main disadvantage of this scheme is the relative low power density of the buck converter due to use of L and C elements in comparison with the other circuits that only use semiconductors for power conversion. The proposed system was analyzed based on the assumption that the rectifier operates under constant load current. Under these conditions, the output voltage $V_S$ is given by

$$V_s = \frac{3\sqrt{6}}{\pi} \cdot V_{rms} - V_r - V_\gamma \tag{1}$$

where $V_{rms}$ is the rms phase voltage of the machine and $V_r$ and $V\gamma$ are the resistive voltage drop on the switches and the voltage loss due to current commutation, respectively. By assuming common values for the voltage drops, the required rms voltage of the generator can be computed. The currents on the ac side are imposed by the rectifier operation and are rectangular. The rms value of the current and the apparent power of the machine can be found by using the power balance of the system at steady state.

## III. Generator Design

### A. Machine Topology

The rotor structure of the machine addressed in this paper is the surface-mounted magnet type as shown in Fig. 2.

The main advantage of this topology is that all of the magnetic flux produced by the magnets links the stato, and therefore, takes part in energy conversion. The design uses arc magnets glued on the rotor to prevent them coming off at high speeds. Additional magnet retention can be provided using wire wrapping, stainless steel, or mylar sleeve. The winding is distributed so that the output voltage of the machine is close to a sine wave.

### B. List of Symbols

| | |
|---|---|
| $n$ | machine speed; |
| $f$ | frequency; |
| $\gamma$ | angle between two consecutive slots; |
| $\alpha$ | short pitching angle; |
| $\sigma$ | skewing angle; |
| $E_{pk}$, $I_{pk}$ | peak values of the back emf and current; |
| $B_{sat}$ | iron saturation flux density; |
| $D_i$ | inner stator diameter; |
| $\mu_r$ | recoil permeability of the magnet; |
| $C_\Phi$ | flux concentration factor; |
| $\tau_p$ | rotor pole pitch; |
| $\tau_s$ | stator slot pitch; |
| $w_s$ | slot width; |
| $t_t$ | tooth width; |
| $k_{st}$ | lamination stacking factor; |
| $k_{sf}$ | slot filling factor; |
| $\rho_{\text{co}}\theta$ | copper electric resistivity; |
| $V_t$ | tooth volume; |
| $V_y$ | yoke volume; |
| $\Gamma_t$, $\Gamma_y$ | iron-specific losses (W/kg); |
| $N_s$ | number of slots; |
| $A_{slot}$ | slot area; |
| $K_{fb}$ | friction coefficient; |
| $W_r$ | rotor weight; |
| $\Re_k$ | sector $k$ magnet reluctance; |
| $\Re_{g,k}$ | sector $k$ air-gap reluctance; |
| $\Phi_k$ | sector mesh flux; |
| $\Phi_{m,k}$ | sector $k$ magnet flux; |
| $\Phi_{g,k}$ | sector $k$ air-gap flux; |
| $mmf_k$ | sector $k$ stator $mmf$; |
| $R_I$ | stator inner radius; |
| $g_k$ | sector $k$ air-gap length; |
| $B_{g,k}$ | sector $k$ air-gap flux density; |
| $A_k$ | sector $k$ air-gap area; |
| $\Delta\theta_k$ | angular width of sector $k$; |
| $\theta_k$ | angle where sector $k$ is centered; |
| $\theta_{esi}$ | initial angle of the phase currents; |

### C. Description of the Design Algorithm

The design starts with a set of initial data that includes the material data of the magnet, iron, and conductors. The number of pole pairs $p$ and the number of slots/pole/phase $q$ are user defined between minimum and maximum bounds. For each set of $(p, q)$, the distribution, short-pitching, and skewing factors $(k_d, k_{sp}, k_s)$ are computed

$$k_d = \frac{\sin\left(\frac{q\gamma}{2}\right)}{q \cdot \sin\left(\frac{\gamma}{2}\right)} \tag{2}$$

$$k_{sp} = \cos\left(\frac{\alpha}{2}\right) \tag{3}$$

$$k_s = \frac{\sin\left(\frac{\sigma}{2}\right)}{\frac{\sigma}{2}}. \tag{4}$$

The winding factor $k_w$ is

$$k_w = k_d \cdot k_{sp} \cdot k_s. \tag{5}$$

The rotor diameter $D$ and the slot depth $d_s$ are iterated between their minimum and maximum specified. The nature of the application requires minimum machine volume. By examining the expression of the air-gap power (6) [9], minimum volume is obtained when the product of the electric and magnetic loading ($AB_g$) is maximized

$$P_{gap} = 4k_p k_i k_w \sin\left(\alpha_m \frac{\pi}{2}\right) \frac{f}{p} (A \cdot B_g) \cdot D^2 L \tag{6}$$

where the power and current waveform factors $k_p$ and $k_i$ are given by (7) and (8)

$$k_p = \frac{1}{T} \int_0^T \frac{e(t)i(t)}{E_{pk} I_{pk}} dt \tag{7}$$

$$k_i = \frac{I_{pk}}{I_{rms}}. \tag{8}$$

The maximization of the product $B_g A$ is a complex problem because the attempt to increase one term results in the decrease of the other. For example, an increase of the air-gap flux density $B_g$ in the machine requires wider tooth in order to avoid saturation. Consequently, the space allocated for conductors and the ampere loading $A$ are reduced. One of the results presented in [10] is used to define the stator structure that will produce a minimum volume machine.

In most electric machine applications, $0.5\tau_s < w_s < 0.6\tau_s$ and

$$t_t = (1 - w_s) \cdot \tau_s. \tag{9}$$

In this analysis, we will make the approximation of equal slot and tooth width

$$w_s \approx t_t. \tag{10}$$

The next task is to determine the pole pitch coverage coefficient of the magnet $\alpha_m$ and the radial length $l_m$ that conducts to this structure. The radial length $l_m$ and $C_\Phi$ are

$$l_m = g \cdot C_\Phi \cdot PC \tag{11}$$

$$C_\Phi = \frac{2 \cdot \alpha_m}{1 + \alpha_m}. \tag{12}$$

The air-gap length $g$ is usually determined by mechanical constraints and is a given data. The permeance coefficient (PC) represents the slope of the air-gap line in the second quadrant of the B-H plane. This is a measure of the capacity of the magnet to withstand demagnetization and must be carefully chosen. According to [5], a permeance coefficient of $5 \sim 20$ guarantees a successful design. The lowest value was adopted in order to minimize the magnet cost.

The value of the flux density in the air gap, $B_g$, is

$$B_g = \frac{C_\Phi}{1 + \frac{\mu_r k_c k_{ml}}{PC}} B_r \tag{13}$$

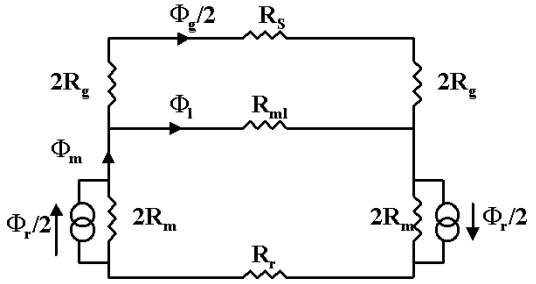


Fig. 3. Magnetic equivalent circuit of the PM machine.

where Carter's factor $k_c$ and the magnetic leakage coefficient $k_{ml}$ are described by (14) and (15)

$$k_c = \left[1 - \frac{w_s}{\tau_s} + \frac{4\left(g + \frac{l_m}{\mu_r}\right)}{\pi \tau_s} \ln\left(1 + \frac{\pi w_s}{4\left(g + \frac{l_m}{\mu_r}\right)}\right)\right]^{-1} \tag{14}$$

$$k_{ml} = 1 + \frac{4 l_m}{\pi \mu_r \alpha_m \tau_p} \ln\left[1 + \pi \frac{g}{(1 - \alpha_m)\tau_p}\right]. \tag{15}$$

Tooth width $t_t$ is given by

$$t_t = \frac{\pi D_i}{k_{st} N_s} \cdot \frac{B_g}{B_{sat}} \tag{16}$$

and to get minimum volume, this must be half of the stator slot pitch. After inserting (13), (16) is nonlinear in $\alpha_m$ and is difficult to solve. The value of $\alpha_m$ is found iteratively. An initial value is chosen for $\alpha_m$ and the air-gap flux density and the tooth width are computed. Condition (10) is checked and $\alpha_m$ is adjusted until this is met. The method mentioned before ensures that the machine stator is well dimensioned in terms of saturation and minimum resulting volume. The magnet radial length can then be computed using (11). An interesting result is that this structure cannot be obtained if a low-energy magnet is used. The tooth of the machine will be magnetically under loaded if

$$B_{g_{\alpha_m = 1}} \leq B_{sat} \frac{k_{st}}{2} \tag{17}$$

and the stator structure cannot be optimized according to this criterion.

Once $\alpha_m$ and $B_g$ are set, the dimensions of the stator yoke $y_t$ and rotor core $y_{rt}$ are found

$$y_t = \frac{\pi D_i \alpha_m}{4 k_{st} p} \cdot \frac{B_g}{B_{sat}} \tag{18}$$

$$y_{rt} = \frac{\pi (D - 2 \cdot l_m) \cdot \alpha_m}{4 k_{st} p} \cdot \frac{B_g}{B_{sat}}. \tag{19}$$

The outer diameter of the machine OD is

$$OD = D + 2(g + d_s + y_t). \tag{20}$$

The expression of the air-gap flux density (13) is presented in [3]. This was derived based on the magnetic model presented in Fig. 3, where the iron reluctances $R_r$ and $R_s$ are neglected.

In this stage, the flux density can be updated to take into account the $mmf$ drops on the iron as the magnetic circuit was

already established. This procedure is based on Ampere's law and the assumption that the flux lines travel on the average path. Iron magnetization characteristic is modeled using "spline" interpolation. An updated value $B_{g-\text{nonlin}}$ is obtained. The flux density in the teeth, stator yoke, and rotor core of the machine are recomputed, and will be used to determine core losses.

Power balance is used to determine the machine length $L$. For a generator

$$P_{gap} = P_{copper} + P_{core} + P_{out} \tag{21}$$

$$P_{copper} = \rho^{\theta}_{Co} N_s J^2 k_{sf} d_s w_s \left( \frac{L}{\cos\sigma} + \frac{2D}{p} \right) \tag{22}$$

$$P_{core} = \rho_{iron} k_{st} \left( N_s V_t \Gamma_t + V_y \Gamma_y \right) \tag{23}$$

$$P_{out} = S \cdot pf. \tag{24}$$

The ampere loading in (6) can be put as

$$A = \frac{6 N_{coils} I_{rms}}{\pi D_i} \tag{25}$$

and the current density $J$ in the conductors is

$$J = \frac{6 N_{coils} I_{rms}}{k_{sf} N_s A_{slot}}. \tag{26}$$

A two-layer winding has been used in this design. This solution is the most used in ac machines. The number of coils per phase $N_{coils}$ is

$$N_{coils} = 2pqN. \tag{27}$$

The number of turns per coil $N$ is an important parameter of the design in terms of machine loading and back electromotive-force (emf) production. Increase of $N$ results in a high electric loading of the machine that requires a reduced length. $N$ is iterated and (21) is solved each time to find the machine length $L$. The copper losses and the core losses as well as the air-gap power are a linear function of $L$. Thus, a set of designs is obtained. The diameter of the conductor in the winding is found by

$$d_c = \sqrt{\frac{2 N_s k_{sf} A_{slot}}{3\pi N_{coils}}}. \tag{28}$$

The friction and windage losses are considered in order to compute the efficiency. The expressions for losses (in Watts) are given by Gieras *et al.* [2]

$$P_f = K_{fb} W_r n \cdot 10^{-3} \tag{29}$$

$$P_w = 2D^3 L n^3 \cdot 10^{-6}. \tag{30}$$

A large set of possible designs is obtained at this stage. Various constraints can be used to select the design that best fits the application. For the case of the PM alternator, the design with the maximum efficiency was selected.

### D. Temperatures

One of the biggest disadvantages of the NdFeB magnet is the dependance of its remanent flux density with temperature. The temperature coefficient of $B_r$ is negative (in the range of 0.07–0.13%/°C), thus, the accuracy of design can be influenced. The electric resistivity of the conductors and the copper losses are also a function of temperature. An analytical thermal model to allow the computation of the magnet and winding temperatures is usually difficult to develop and involves many uncertainties. The model structure as well as thermal parameters of the materials used can easily conduct to severe errors. Reference [10] considers that a reasonable assumption for the magnet and winding steady-state temperature is

$$T_{magnet} = T_{ambient} + (20 \sim 30)^{\circ}\text{C} \tag{31}$$

$$T_{winding} \leq 110^{\circ}\text{C}. \tag{32}$$

### E. Armature Reaction

The design method presented neglects armature reaction. The effect of the stator currents on the magnetic field of the machine is generally very small in PM machines. The low recoil permeability of the magnets and their long relative length make the stator field see an increased air gap. Typically, the magnitude of the armature reaction flux density is no bigger than 10% of that produced by the magnets.

### F. Input Data and Design Results

The design input data and the design results are shown in Tables I and II.

## IV. Reluctance Model

An alternative magnetic equivalent model of the PM machine was developed, which is called "reluctance model." The model takes into account the effect of $mmf$ caused by stator currents as shown in Fig. 4. The machine can be sectionalized in radial direction by stator slots. Thus, $N_s$ sectors are obtained, each sector being centered on a stator slot. The magnet section of each sector is represented in the model by a flux source in parallel with a reluctance. Similar technique for analyzing a transformer in three dimension (3-D) can be seen in [11].

The sinusoidal distributed stator $mmf$ was made equivalent to a concentrated $mmf$ which is the integral of the equivalent stator current sheet over the appropriate arc. The model components for sector number $k$ are

$$\Phi_{m_k} = B_r A_{m_k} \tag{33}$$

$$\Re_k = \frac{l_m}{\mu_0 \mu_r A_m} \tag{34}$$

$$\Re_{g_k} = \frac{g_k}{\mu_0 L R_i \Delta\theta_k} \tag{35}$$

$$mmf_k = 6\frac{\pi}{p} k_w N_{coils} I_{rms} \Delta\theta_k \cdot \cos\left[ p\left( \frac{\pi}{2} + \theta_{esi} - \theta_k \right) \right]. \tag{36}$$

The model can be transposed using Norton-Thevenin theorem and the circuit obtained is solved for the mesh fluxes $\Phi_1, \Phi_2, \ldots, \Phi_{\text{Ns}}$. The flux crossing the air gap and the corresponding flux density for sector $k$ are

$$\Phi_{g_k} = \Phi_k - \Phi_{k+1} \tag{37}$$

$$B_{g_k} = \frac{\Phi_{g_k}}{A_k}. \tag{38}$$

TABLE I
DESIGN INPUT DATA

| | |
|---|---|
| Apparent power, S | 3 kVA |
| Phase voltage, $V_{rms}$ | 20V |
| Phase current, $I_{rms}$ | 50 A |
| Power factor, pf | 0.854 |
| Speed, n | 1800 rpm |
| Power waveform factor, $k_P$ | 0.554 |
| Current waveform factor, $k_i$ | 1.224 |
| Stacking factor, $k_{st}$ | 0.94 |
| Slot filling factor, $k_{sf}$ | 0.4 |
| Short pitching | 1 slot |
| Skewing | 0 |
| Magnet: MQ3G 32SH | |
| Remanent flux density | 1.16 T |
| Temp. coefficient of $B_r$ | -0.009%/°C |
| Iron: type 1008, unannealed | |
| $B_{sat}$ | 1.7 T |
| $T_{ambient}$ | 20°C |
| $T_{magnet}$ | 50°C |
| $T_{winding}$ | 110°C |

TABLE II
DESIGN RESULTS

| | |
|---|---|
| No. of pole pairs ,p | 2 |
| No. of slots/pole/phase, q | 2 |
| Rotor diameter, D | 90 mm |
| Outer diameter, OD | 165 mm |
| Machine length, L | 124.1 mm |
| Magnet length, $l_m$ | 3.3 mm |
| Coverage coefficient, $\alpha_m$ | 0.795 |
| Slot depth $d_s$ | 22.5 mm |
| Tooth width $t_t$ | 5.97 mm |
| Slot width, $w_s$ | 5.99 mm |
| Stator yoke thickness, $y_t$ | 14.2 mm |
| Rotor core thickness, $y_{rt}$ | 12.99 mm |
| Air gap flux density | 0.797 T |
| No. of coils per phase | 16 |
| No. of turns per coil | 2 |
| Total ampere loading, A | 16698 A/m |
| Current density, J | 3.7 A/mm$^2$ |
| Air gap power, $P_{gap}$ | 2813.44 W |
| Core losses, $P_{core}$ | 162.59 W |
| Copper losses, $P_{copper}$ | 88.85 W |
| Rotational losses | 27.64 W |
| Output power, $P_{out}$ | 2562 W |
| Efficiency | 0.9017 |
| Conductors | AWG 17 |

Finally, the air-gap flux density in the machine is computed by taking the average over one pole. The model was simulated for the design presented. For $\theta_{esi} = 90°$, the air-gap flux density obtained was 0.742 T.

## V. DESIGN VALIDATION

The design presented in section III was checked for saturation using a finite-element analysis (FEA) package–Magsoft Flux2D. Magnetostatic simulations were used for the generator at no load and full load. Even though 3D FEA technique is available for better performance [12], 2D FEA is faster and accurate enough to validate the performance of the "reluctance model." The distribution of flux lines and the magnitude of the flux density in the machine for no-load conditions are shown in Figs. 5 and 6.

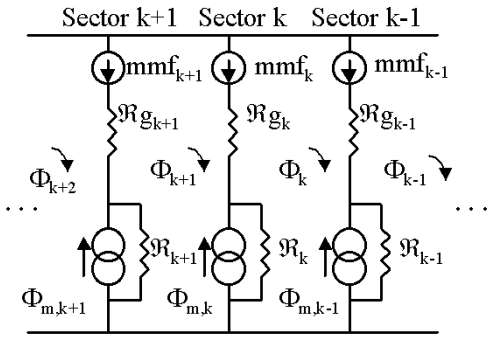


Fig. 4. Reluctance model of the PM machine.

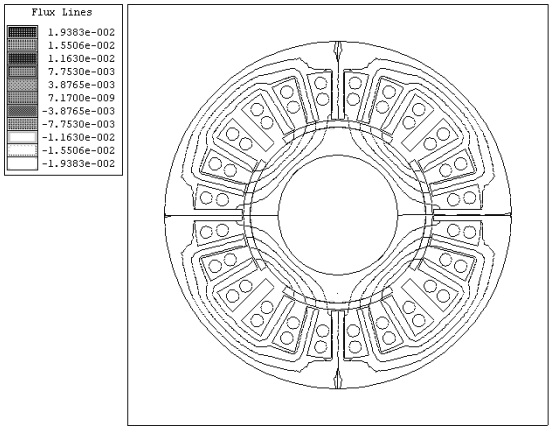


Fig. 5. Flux lines in the PM generator at no load (numbers are in weber).

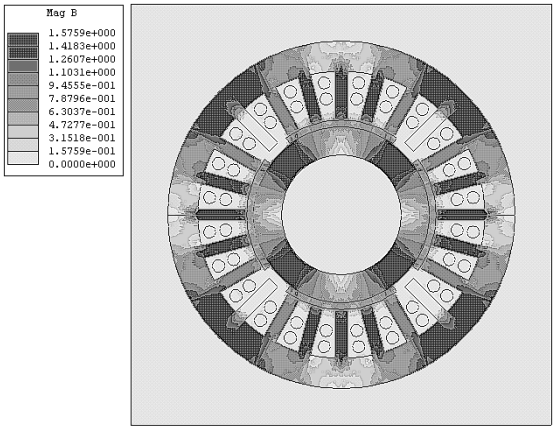


Fig. 6. Magnitude of the flux density in the machine at no load.

The value of the flux density was checked in various points of the teeth, stator yoke, and rotor core of the machine. As shown in Table III, results are close to those obtained analytically.

The flux density distribution in the PM generator at full load is shown in Fig. 7. The effect of stator currents is an increase of the value of $B$ and a distortion of the field compared to the no load case. The results obtained show that the iron sections of the machine are not saturated. The maxiumum flux density obtained for the full-load case is approximately 1.65 T while the saturation value of the iron had been set at 1.7 T.

TABLE III
MAGNITUDE OF THE FLUX DENSITY IN DIFFERENT REGIONS OF THE MACHINE

| B (Tesla) | Analytical | No load | Full load |
|---|---|---|---|
| Teeth | 1.538 | 1.575 | 1.653 |
| Yoke | 1.538 | 1.552 | 1.617 |
| Core | 1.538 | 1.563 | 1.646 |

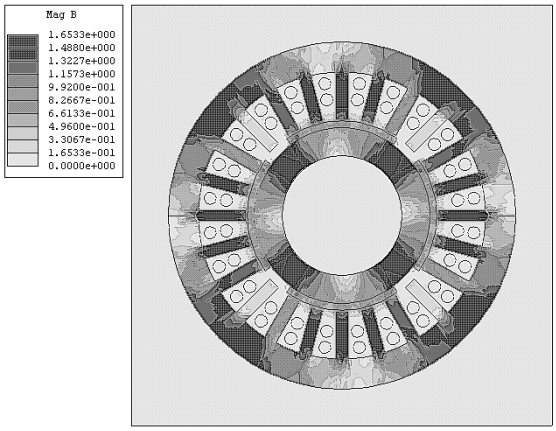


Fig. 7. Magnitude of the flux density in the PM generator at full load.

## VI. CONCLUSIONS

A design method for a PM generator is presented. The generator is to be used as an alternator in the electric system of an automobile. Input data and design results are shown. An alternative analytical magnetic circuit model of the PM machine called the "reluctance model" has been developed. This is based on machine sectionalizing and accounts for armature reaction. The proposed design based on the analytical approach has been checked for saturation using finite-element analysis. The validation results demonstrate the effectiveness of the proposed analytical machine design topology.

## REFERENCES

[1] K. J. Binns and D. W. Shimmin, "The relationship between performance characteristics and size of permanent magnet motors," in *Proc. 1995 Elect. Mach. Drives Conf.*, pp. 423–427.
[2] J. F. Gieras and M. Wing, *Permanent Magnet Motor Technology, Design and Applications*. New York: Marcel Dekker, 1997.
[3] D. C. Hanselmann, *Brushless Permanent Magnet Motor Design*. New York: McGraw-Hill, 1994.
[4] S. Huang, J. Luo, F. Leonardi, and T. Lipo, "A general approach to sizing and power density equations for comparison of electrical machines," *IEEE Trans. Energy Conversion*, vol. 34, pp. 92–97, Mar. 1998.
[5] J. R. Hendershot and T. J. E. Miller, *Design of Brushless Permanent Magnet Motors*. Oxford, U.K.: Magna Physics Publishing and Clarendon Press, 1994.
[6] I. Khan, "Power electronics in automotive electrical systems," in *IEEE Workshop Power Electron. Transportation*, 1996, pp. 29–38.
[7] P. R. Nicastri and H. Huang, "Jump starting 42 V powernet vehicles," *IEEE Aerosp. Electron. Syst. Mag.*, vol. 15, pp. 25–31, Aug. 2000.
[8] P. Pillay and P. Freere, "Literature survey of permanent magnet AC motors and drives," *IEEE IAS Annu. Meeting Conf. Rec.*, pt. 1, pp. 74–84, Oct. 1989.
[9] T. A. Lipo, *Introduction to AC Machine Design*. Madison, WI: Univ. Wisconsin, Wisconsin Power Electronics Research Center, 1996, vol. 1.
[10] T. Sebastian, "Temperature effects on torque production and efficiency of PM motors using NdFeB magnets," *IEEE Trans. Ind. Applicat.*, vol. 31, pp. 353–357, Mar./Apr. 1995.
[11] J. Turowski, M. Turowski, and M. Kopec, "Method of three-dimensional network solution of leakage field of three-phase transformers," *IEEE Trans. Magn.*, vol. 26, pp. 2911–2919, Apr. 1990.
[12] M. A. Alhamadi and N. A. Demerdash, "Modeling and experimental verification of the performance of a skew mounted permanent magnet brushless DC motor drive with parameters computed from 3D-FE magnetic field solutions," *IEEE Trans. Energy Conversion*, vol. 9, pp. 26–35, Mar. 1994.

**Mihai Comanescu** (S'02) received the electrical engineer diploma from Politehnica University of Bucharest, Bucharest, Romania, in 1992. Currently, he is pursuing the M.S.E.E. degree with the Department of Electrical Engineering at The Ohio State University, Columbus.

Mr. Comanescu's research interests are permanent-magnet machine design, modeling, and parameter estimation.

**Ali Keyhani** (F'98) is the director of the Department of Electrical Engineering Mechatronic Systems Laboratory, The Ohio State University, Columbus. He established The Ohio State University Mechatronic graduate program in 1995. His research interests are in the areas of mechatronic/electromechanical systems, power systems, hybrid electric vehicles, power electronics, design of electric machines, finite-element modeling, digital signal processing, parameter estimation, and control of electromechanical systems.

Dr. Keyhani is the Chairman of the Electric Machinery Committee and the past Editor of IEEE TRANSACTIONS ON ENERGY CONVERSION. He has been a consultant to Accuray, Combustion Engineering, Asea Brown Boveri, TRW Controls, Harris Controls, Liebert, Delphi Automotive Systems, Mahab Engineering, IRD, and Foster Wheeler Engineering. He has authored many papers in the IEEE Transactions on control of power systems, machine modeling, parameter estimation, power electronic systems, design of virtual and test beds for variable speed drive systems. He was a recipient ofThe Ohio State University College of Engineering Research Award for 1989 and 1999.

**Min Dai** (S'99) was born in Shanghai, China, in 1971. He received the B.S. and M.S. degrees in electrical engineering from Tsinghua University, Beijing, China, in 1994 and 1997, respectively. He also received the M.S. degree in computer science from the University of Alabama, Huntsville, in 1999.

From 1993 to 1997, he worked in the State Key Lab of Intelligent Technology and Systems at Tsinghua University on robotics and intelligent control. From 1997 to 1999, he was a research assistant in the Visualization Lab at the University of Alabama, Huntsville, working on computer vision and 3-D object recognition. He joined the Department of Electrical Engineering at The Ohio State University as a Ph.D. student in 1999. His current research at The Ohio State University includes electrical machines and variable speed drives, control in power electronic systems, and distributed power systems.